J Dent Sci 2009;4(3):118–129

ORIGINAL ARTICLE

Improving the video imaging prediction of postsurgical facial profiles with an artificial neural network

Chien-Hsun Lu,[1,2] *Ellen Wen-Ching Ko,*[3,4] *Li Liu*[5]*

[1]Department of Dentistry, Taipei Medical University–Shuang Ho Hospital, Taipei, Taiwan
[2]Department of Dentistry, Mackay Memorial Hospital, HsinChu, Taiwan
[3]Graduate Institute of Craniofacial and Oral Science, Chang Gung University, Taipei, Taiwan
[4]Department of Craniofacial Orthodontics, Chang Gung Memorial Hospital, Taipei, Taiwan
[5]Graduate Institute of Medical Informatics, Taipei Medical University and Taipei Medical University Hospital, Taipei, Taiwan

Received: May 10, 2009
Accepted: Aug 13, 2009

KEY WORDS:
artificial neural network;
improvement;
orthognathic surgery;
prediction;
video image

Background/purpose: With advancements in computer technology, postsurgical video image simulations are becoming more frequently used in orthognathic surgery. Simulations can greatly affect decision making by patients and also provide information to surgeons and orthodontists. However, most of the current commercial video image prediction software is only suitable for patient education but is not precise enough for clinical communication and treatment planning. The purpose of this study was to evaluate and improve post-orthognathic surgery image predictions.
Materials and methods: In this retrospective study, 30 bimaxillary protrusion patients who underwent two jaw surgeries were recruited. Simulations were compared with the actual postsurgical facial profile. An artificial neural network (ANN) was used to improve the predictions.
Results: The lower lip was the least accurate point, and the prediction error on the sagittal plane was +4.0 mm. After applying the ANN to the input data, the prediction error was reduced to +0.3 mm with a >80% improvement rate. The overall probability of the prediction errors being <2 mm was 52% before improvement and 84.5% after improvement. Improvement rates of the average prediction errors on the sagittal and vertical planes were 43.9% and −6.6%, respectively.
Conclusion: With the help of an ANN, the accuracy and reliability of the postsurgical profile video image predictions were greatly improved to a clinically applicable and treatment planning level.

Introduction

Facial esthetic improvement is the main reason patients seek surgical correction of dentofacial deformities.[1] However, the definition of an ideal result for facial improvement after surgical orthodontic treatment is very subjective. Therefore, prevision of the improvement has become an important issue

*Corresponding author. Graduate Institute of Medical Informatics, Taipei Medical University and Taipei Medical University Hospital, c/o College of Public Health, National Taiwan University, Room 438, 4 F, 17, Xu-Zhou Road, Taipei 100, Taiwan.
E-mail: davidliliu@gmail.com

Table 1. Literature review of the least accurate area in software prediction of facial soft tissue changes after orthognathic surgery

Author	Least accurate	Predicted error (mm)	Sample size	Type of surgery	Software
Lu et al.[16]	Lower lip Upper lip	+4.0±2.3 (H) +1.7±2.4 (V)	30	Wassmund maxillary setback Köle mandibular setback	DI
Kazandjian et al.[18]	Upper lip Lower lip	+2.25±3.63 (H) −2.23±2.85 (V)	30	Mandibular setback	QC, PoP
Sameshima et al.[19]	Lower lip	+1.71±1.37 (H) +2.88±2.62 (V)	32	Maxillary impaction	OTP, PrP
Syliangco et al.[20]	Lower lip	+1.61±1.24 (H) +1.77±1.26 (V)	39	Mandibular advancement	OTP, PrP
Konstiantos et al.[21]	Lower lip Pronasal	+1.57±2.0 (H) −1.64±1.4 (V)	21	LeFort I osteotomy	DP
Hing[22]	Lower lip Chin	+1.9±0.38 (H) −0.5±0.78 (V)	16	Mandibular advancement	QC

+ = indicates that the predicted landmark was anterior (horizontal) or inferior (vertical) to the actual one; H = horizontal plane; V = vertical plane; DI = Dolphin Imaging; − = indicates that the predicted landmark was posterior (horizontal) or superior (vertical) to the actual one; QC = Quick Ceph (Orthodontic Processing, CA, USA); PoP = Portrait Planner (Rx Data Inc., TN, USA); OTP = Orthognathic Treatment Planner (Pacific Coast Software, CA, USA); PrP = Prescription Portrait (Rx Data Inc.); DP = Dentofacial Planner (Dentofacial Software, Toronto, Ontario, Canada).

among patients, surgeons, and orthodontists.[2,3] Several measures were proposed to predict the post-surgical facial profile.[4–7] With advancements in digital imaging technology, profile predictions are generated by computer.[8–15] However, the accuracy and reliability of these simulations and the results are often not very satisfactory (Table 1).[16–23] Most authors suggest that current simulation programs are good for patient education but not accurate enough for treatment planning. Therefore, it is important to improve the accuracy and reliability of video image simulations. However, during a literature review, no articles related to improving post-surgical profile video imaging predictions were found. A new methodology should be developed to improve video simulations.

Artificial intelligence is a branch of computer science capable of analyzing complex medical data. Its potential to exploit meaningful relationships within a dataset can be used for diagnosis, treatment, and predicting outcomes in many clinical scenarios.[24] Artificial neural networks (ANNs) are biologically inspired computer programs designed to simulate the way in which the human brain processes information.[25] They are systems that can learn; in most situations, an operator trains the system with a set of input and output data belonging to a particular category. If new data of the same category but beyond the training set are presented to the system, the network can use the learned data to predict outcomes with no specific programming related to the category of events involved.[26]

We propose that ANNs possess the ability to improve post-orthognathic surgery image predictions. The purpose of this study was to evaluate video image predictions after orthognathic surgery and improve them with an ANN.

Materials and methods

This research was based on a previous study published by Lu et al.[16] in 2003. The samples consisted of 30 adult patients who met the following criteria: (1) having no congenital craniofacial deformities; (2) having no head or neck trauma or surgical history; and (3) having undergone the Wassmund procedure to set back the anterior maxilla and the Köle procedure to set back the anterior mandible with or without genioplasty.

Lateral cephalometric radiographs and profile photographs were taken within 6 months before surgery and at least 6 months after surgery. The head films and photographs were acquired in the natural head position with the teeth in centric occlusion and the lips in a relaxed posture. There were no fixed orthodontic appliances shown on either the head films or photographs.

Evaluating the prediction

An (x, y) coordinate system was set up in order to evaluate the accuracy of the prediction (Fig. 1). The SN plane was defined as the horizontal reference

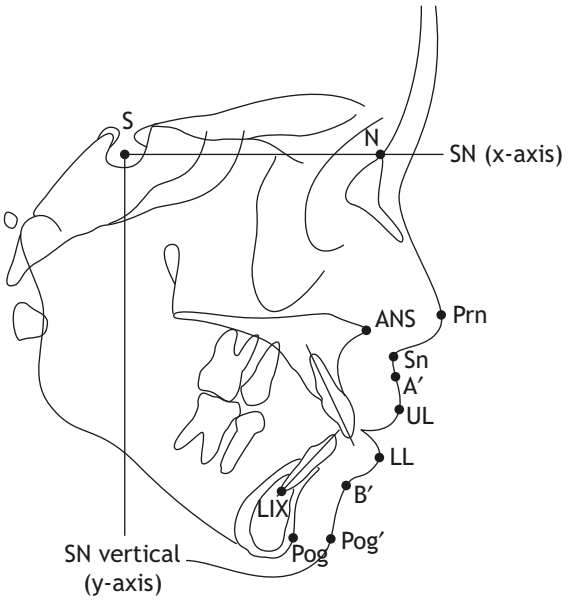

Fig. 1 Cephalometric landmarks used in this study. A′= soft-tissue A point; B′=soft-tissue B point; LIX=lower incisal apex; LL=lower lip; N=nasion; Pog=pogonion; Pog′=soft-tissue pogonion; Prn=tip of the nose; S=sella; Sn=subnasale; UL=upper lip.

plane (x-axis), and a line perpendicular to this plane through the sella was defined as the vertical reference plane (y-axis). Hard-tissue landmarks recorded included the anterior nasal spine (ANS), lower incisor root apex (LIX), and pogonion (pog). The angle of the upper incisor to the SN plane and the lower incisor mandibular plane angle were also recorded. Soft-tissue landmarks recorded included the tip of the nose (Prn), subnasale (Sn), soft-tissue A point (A′), upper lip (UL), lower lip (LL), soft-tissue B point (B′), and soft-tissue pogonion (Pog′). Tracings of the presurgical and postsurgical cephalograms were superimposed at the cranial base to ensure that the (x, y) planes were accurately transferred. The tracings and photographs were then input into the computer, digitized, and superimposed following the instructions of the prediction software (Dolphin Imaging version 6; Dolphin Imaging & Management Solutions, Chatsworth, CA, USA). The perpendicular distances of each landmark to both reference planes (x- and y-axes) were recorded before and after surgery. Treatment changes of hard tissues in each case were obtained from the differences between the pre- and postsurgical linear measurements. The hard-tissue image was moved according to the prescribed distances (the treatment change) using these calculations and the visual treatment objective function in the software. A predicted postsurgical video image was thus generated. The predicted soft-tissue outline and the corresponding coordinates of the soft tissue were also automatically generated. Differences in the soft-tissue outline between the predicted tracing and the actual profile were compared (error of prediction) to test the accuracy of this software.

Improving the prediction with an ANN

Following the instructions of the prediction software we used in this study, eight specific hard-tissue movements were input into the software to generate the prediction. In addition, we wanted to simplify the improvement procedure and avoid modifying the parameters or even reprogramming the software. So improving the prediction focused on altering the input values to the software.

Twenty of the 30 patients were randomly selected to establish the ANN (Group A) and the other 10 patients were used to verify the improvement (Group B). Manual hard-tissue adjustments were performed by one orthodontist and met the adjustment requirements (Fig. 2). The requirements were the designated soft-tissue point prediction errors of <2 mm in the order of Pog′, LL, B′, UL, A′, Sn, and Prn. When the error of the predicted soft-tissue point was adjusted to the required level, the previous soft-tissue points were rechecked to ensure that the prediction errors were still in an acceptable range (<2 mm). If the requirements were not met after 10 trials, the hard-tissue movements were adjusted to achieve the prediction error of the previous soft-tissue point of <2 mm and the prediction error of the present soft-tissue point was as close to 2 mm as possible. After the adjustment, the adjusted hard-tissue movement was recorded and used as a target set of the ANN. In order to provide a larger training sample size for the ANN, the adjustment procedures were performed three times spaced by at least a 1-week interval. Sixty datasets were provided to train the ANN.

The ANN was created with the software NeuroSolutions version 4.2 (NeuroDimension Inc., Gainesville, FL, USA). The adopted neural network was set up with two hidden layers. Each hidden layer possessed the function of a feed-forward back-propagation learning algorithm and was composed of eight processing elements with the tanh axon (Fig. 3). There were eight input neurons for the original treatment changes in hard tissues (original hard-tissue movement) and eight output neurons for adjusted treatment changes of hard tissues (adjusted hard-tissue movement). The input data included the movements of the ANS on the x- and y-axes, Pog on the x- and y-axes, the angle of upper incisor to SN plane, the lower incisor root apex on the *x*- and y-axes, and the lower incisor mandibular plane angle. The original hard-tissue movements of Group A were used as the learning set. The manually

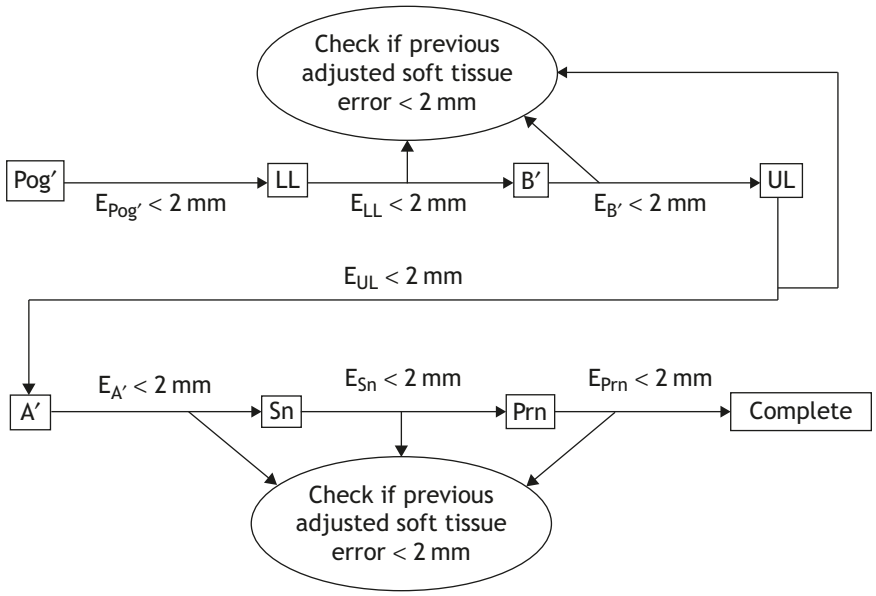

Fig. 2 Adjustment requirement flow chart. A′=soft-tissue A point; B′=soft-tissue B point; E=prediction error; LL=lower lip; Pog′=soft-tissue pogonion; Prn=tip of the nose; Sn=subnasale; UL=upper lip.

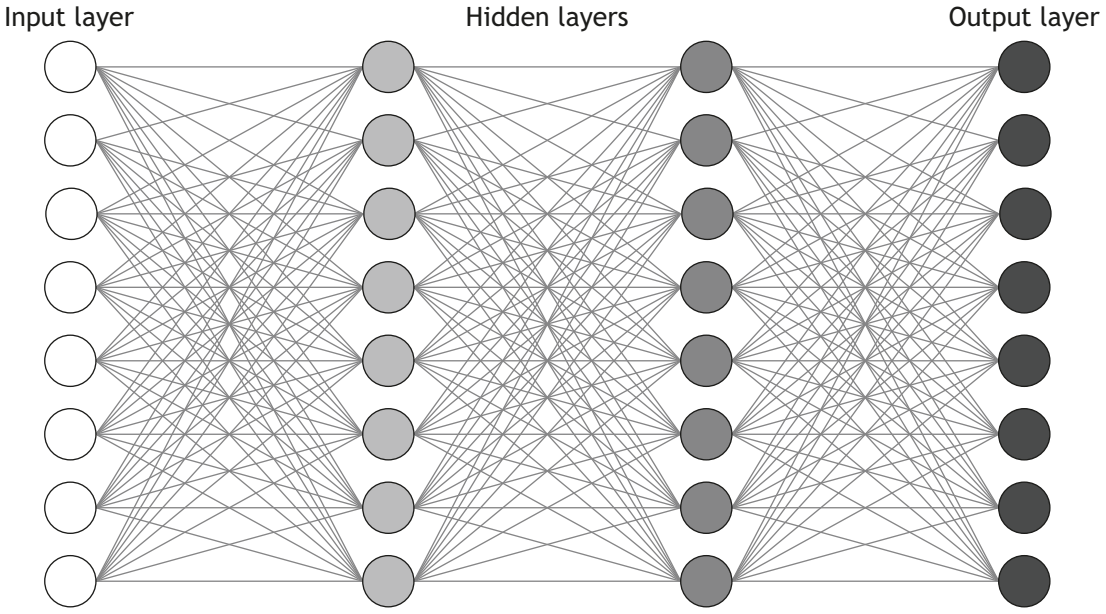

Fig. 3 Architectural graph of the adopted neural network. This network consisted of one input layer, two hidden layers, and one output layer. Each layer possessed eight neurons.

adjusted hard-tissue movements of Group A were used as the target set. The ANN was then trained.

Evaluating the improved prediction

Group B patients were used to test the accuracy of the improvement. The original hard-tissue movements of each patient in Group B were input to the trained ANN, and an adjusted hard-tissue movement was then generated. These new generated values were input to the prediction software, and an improved postsurgical video image prediction was then produced. The prediction errors between the actual final profile and the improved predicted soft-tissue outline were calculated and compared with those without improvement.

Results

Original prediction errors

Data of the original prediction errors were derived from a previous study by Lu et al.[16] When comparing

the landmarks located in the computer-generated prediction with the actual profile change on the sagittal plane (Table 2), mean differences of <1 mm between the two groups were seen in three of seven soft-tissue measurements, including the tip of the nose, soft-tissue A point, and the upper lip. The most accurate region was located at soft-tissue A point. The largest difference was shown in the region of the lower lip. In general, the predictions tended to underestimate the amount of soft-tissue retraction except for the subnasale and soft-tissue pogonion.

When comparing landmarks of the computer-generated prediction with the actual profile changes on the vertical plane, mean differences of <1 mm between the two groups were seen in six of seven soft-tissue measurements, including the tip of the nose, subnasale, soft-tissue A point, the lower lip, soft-tissue B point, and soft-tissue pogonion. The greatest differences were seen in the region of the upper lip with an average of 1.7 mm. The most accurate prediction was located at soft-tissue B point.

When the data were divided into three categories (errors of <1, 1–2, and >2 mm), the frequency of the prediction errors on the sagittal plane (Table 3) presented a wide range of standard deviations (SDs) with a significant bipolar spread, especially in the region of the lower lip. Eighty percent of the predictions had a difference of >2 mm in the lower lip region. The most reliable region of the prediction was located at the tip of the nose, with

Table 2. Prediction errors*

	Sagittal plane		Vertical plane	
	Original prediction† (mm)	Improved prediction (mm)	Original prediction† (mm)	Improved prediction (mm)
Tip of the nose	+0.5±1.2	+0.7±1.5	−0.5±1.5	+0.1±1.8
Subnasale	−1.7±2.1	−2.4±1.1	−0.8±1.5	−1.0±1.4
Soft-tissue A point	+0.1±2.0	0±1.2	+1.0±2.6	+0.2±1.1
Upper lip	+0.8±2.7	+0.6±1.0	+1.7±2.4	+0.6±0.9
Lower lip	+4.0±2.3	+0.8±1.0	+0.3±3.6	−0.1±1.2
Soft-tissue B point	+3.2±3.0	0±1.6	−0.1±3.4	+0.5±1.8
Soft-tissue pogonion	−1.3±3.2	+0.2±0.9	+0.8±3.7	−0.1±0.7

*Data are presented as X (average of differences between the prediction and actual final result)±SD (standard deviation of differences between prediction and actual final result); †data of the original prediction derived from a previous study.[16] + = indicates that the predicted landmark was anterior (sagittal) or inferior (vertical) to the actual one; − = indicates that the predicted landmark was posterior (sagittal) or superior (vertical) to the actual one.

Table 3. Frequency of the prediction errors*

	Sagittal plane						Vertical plane					
	Original prediction† (%)			Improved prediction (%)			Original prediction† (%)			Improved prediction (%)		
	<1 mm	1–2 mm	>2 mm	<1 mm	1–2 mm	>2 mm	<1 mm	1–2 mm	>2 mm	<1 mm	1–2 mm	>2 mm
Tip of the nose	63	27	10	50	30	20	60	20	20	60	20	20
Subnasale	17	27	57	0	50	50	63	13	23	60	20	20
Soft-tissue A point	33	37	30	50	40	10	27	23	50	60	40	0
Upper lip	33	13	53	50	40	10	30	30	40	70	30	0
Lower lip	7	13	80	70	10	20	17	37	47	60	20	20
Soft-tissue B point	13	20	67	20	50	30	23	30	47	60	20	20
Soft-tissue pogonion	23	20	57	70	30	0	10	23	67	80	20	0
Overall‡	27	22	51	44	36	20	33	25	42	64	24	12

*Prediction errors were divided into three categories: errors of <1, 1~2, and >2 mm; †data of original prediction derived from a previous study;[16] ‡the overall value is the average of all prediction errors.

a difference of <1 mm in 63% and <2 mm in 90%. The overall region presented 49% prediction errors of <2 mm on the sagittal plane.

The frequency of prediction errors on the vertical plane was more concentrated when compared with those on the sagittal plane. The most reliable region of prediction was located at the tip of the nose and subnasale with 60% and 63% errors of <1 mm, respectively. The least reliable region was located at the soft-tissue pogonion with only 10% of the prediction errors of <1 mm. The overall region presented 58% of prediction errors of <2 mm on the vertical plane.

The distribution of prediction errors was plotted as scattergrams (Fig. 4). The individual points of the scattergrams were obtained from subtracting the actual final landmarks from the predicted landmarks. The scattergram of the original predictions showed that the prediction error of distribution of the tip of the nose and subnasale was more accurate and concentrated. The tip of the nose, the lower lip, and soft-tissue B point were estimated to be in a more anterior position. The subnasale was estimated to be in a more posterosuperior position. The upper lip was estimated to be in a more inferior position.

Improved prediction errors

When comparing landmarks of the improved computer-generated prediction with the actual profile change on the sagittal plane (Table 2), mean differences of <1 mm between the two groups were seen in six of seven soft-tissue measurements, including the tip of the nose, soft-tissue A point, the upper lip, the lower lip, soft-tissue B point, and the soft-tissue pogonion. The most accurate regions were located at soft-tissue A and B points. The largest differences were shown in the region of the subnasale. In general, the predictions tended to underestimate the amount of soft-tissue retraction except for at the subnasale.

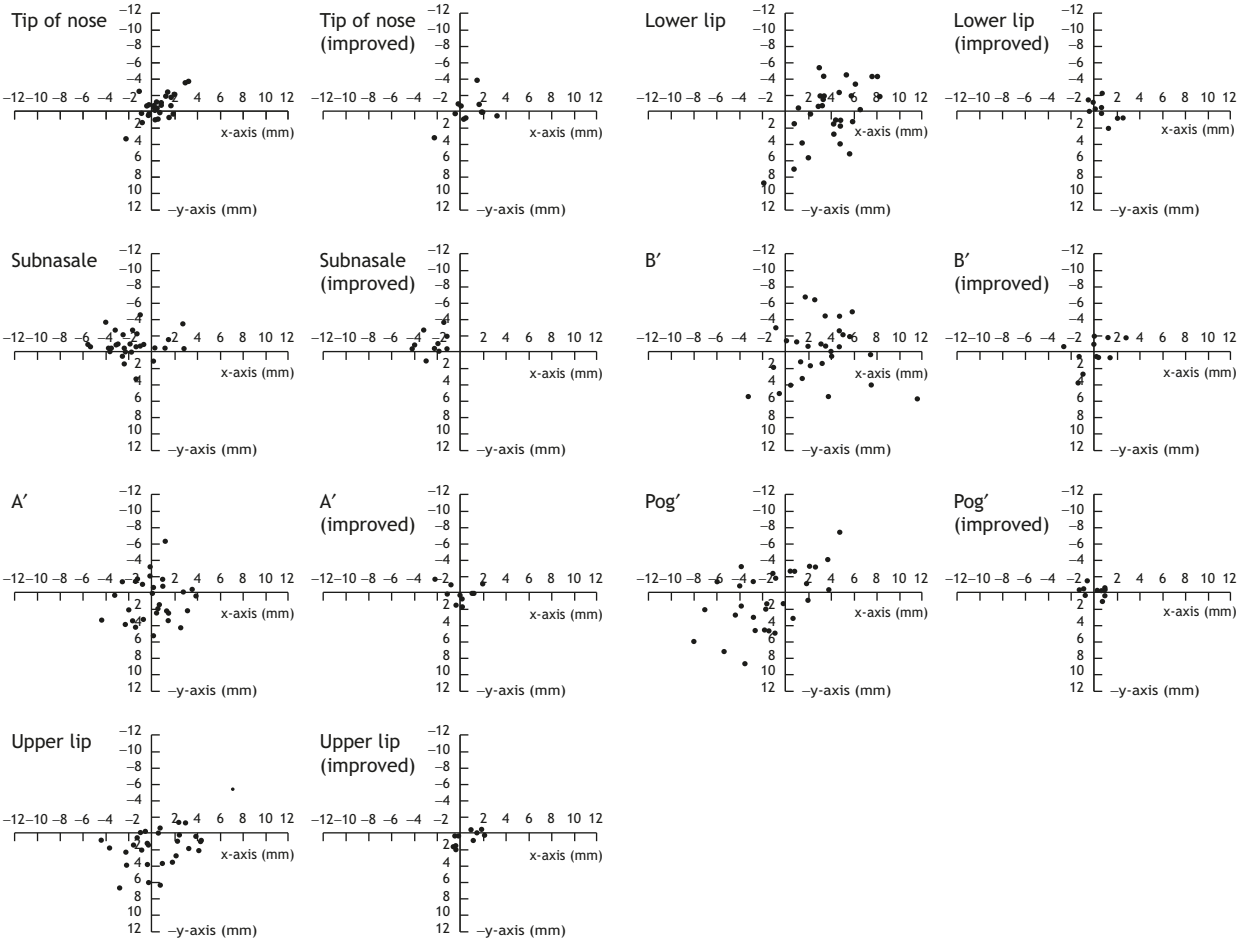

Fig. 4 Scattergrams of the prediction errors. Individual points in the scattergrams were obtained by the coordinates of the predicted landmarks minus those of the actual final landmarks. Positive values indicate that the predicted landmarks were anterior (x-axis) or inferior (y-axis) to the actual ones, while negative values indicate that the predicted landmarks were posterior (x-axis) or superior (y-axis) to the actual ones. Those labeled "improved" were scattergrams with improved predictions. B′ = soft-tissue B point; A′ = soft-tissue A point; Pog′ = soft-tissue pogonion.

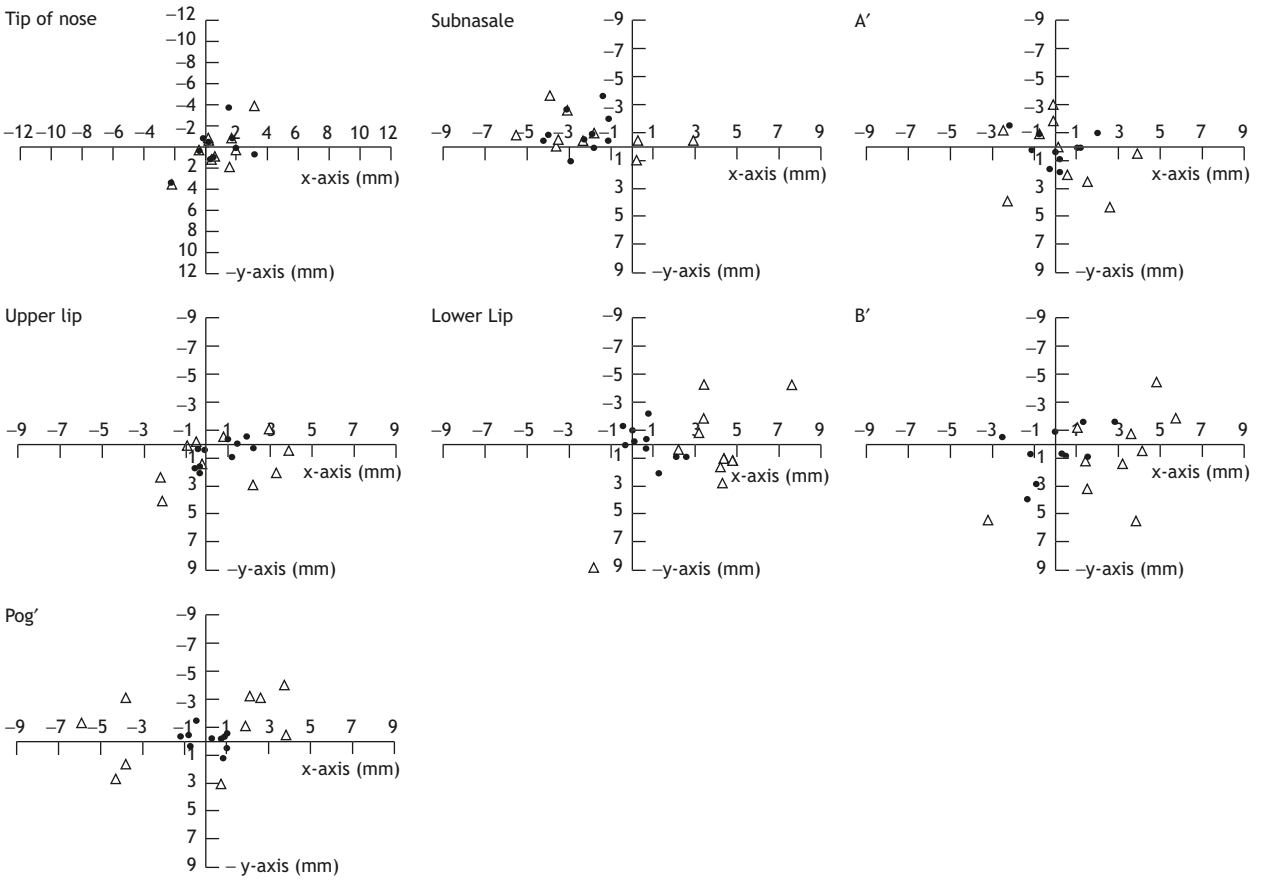

Fig. 5 Scattergrams of the prediction errors of Group B with and without improvement. △=prediction errors without improvement; ●=prediction errors with improvement. A′=soft-tissue A point; B′=soft-tissue B point; Pog′=soft-tissue pogonion.

When comparing landmarks of the improved computer-generated prediction with the actual profile changes on the vertical plane, mean differences of <1 mm between the two groups were seen in six of seven soft tissue measurements, including the tip of the nose, soft-tissue A point, the upper lip, the lower lip, soft-tissue B point, and the soft-tissue pogonion. The greatest differences were seen in the region of the subnasale with an average of 1.0 mm. The most accurate prediction was located at the soft-tissue pogonion.

The frequency of the improved prediction errors (Table 3) of the sagittal plane was located more in the region of <1 mm compared with those without improvement. The most reliable region of the prediction was located at the soft-tissue pogonion, with a difference of <1 mm in 70% and <2 mm in 100%. The second most reliable region was located at the lower lip, with a difference <1 mm in 70% and <2 mm in 80%. The least reliable region of the prediction was located at the subnasale with a difference >2 mm in 50%. The overall region presented 80% of prediction errors of <2 mm on the sagittal plane.

The frequency of prediction errors on the vertical plane was more concentrated when compared with those on the sagittal plane. The most reliable region of prediction was located at the tip of the nose and subnasale with 60% and 63% errors of <1 mm, respectively. The least reliable region was located at the soft-tissue pogonion with only 10% of the prediction errors of <1 mm. The overall region presented 58% of prediction errors of <2 mm on the vertical plane.

After improvement, the scattergrams (Fig. 4) showed that the prediction errors of distribution were more concentrated than those without improvement. The tip of the nose, the upper lip, and the lower lip were estimated to be in a more anterior position. The subnasale was estimated to be in a more posterosuperior position. Soft-tissue B point was scattered around the origin of the coordinates, while the soft-tissue pogonion was distributed near the origin of the coordinates. When comparing the distribution of Group B samples with and without improvement (Fig. 5), we found that the distribution of errors with improvement were more concentrated and also closer to the origin of the coordinates. Because of smaller prediction errors before improvement, the distribution of the scattergram of the tip of the nose with and without

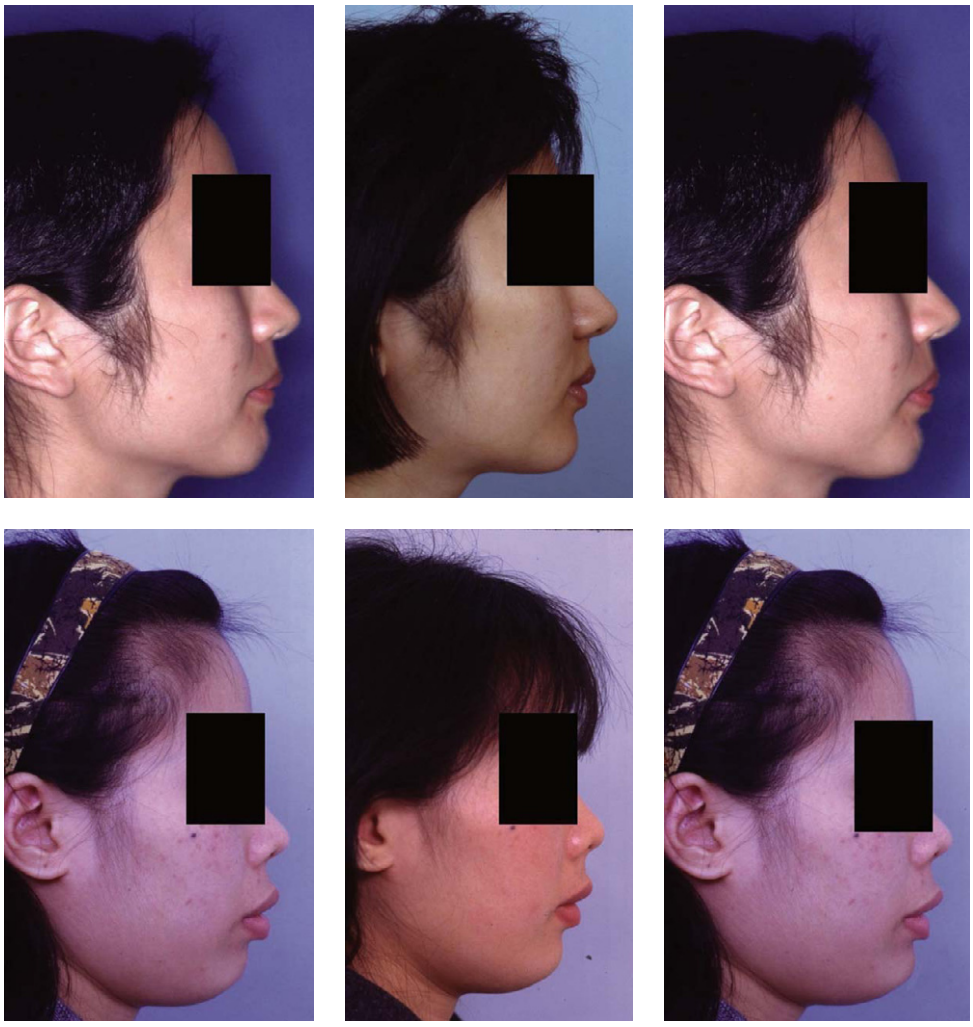

Fig. 6 Two examples of the video prediction and improved video prediction. The computer-generated prediction, actual final image, and improved prediction are represented by the left, middle and right images. Note the differences in the lip region among these images. The improved predictions were more similar to the actual final images.

improvement was similar. The scattergram of the subnasale showed that the prediction errors with improvement were concentrated to the center of those without improvement. The scattergram of the soft-tissue A point, the upper lip, and the soft-tissue pogonion showed that the improved prediction errors were concentrated to the center of those without improvement and were also concentrated to the origin of the coordinates. The scattergram of the lower lip and soft-tissue B point showed that the prediction errors with improvement were concentrated toward the origin of the coordinates.

Examples of predicted profile images, actual postsurgical profiles, and predicted profile images with improvement are presented in Fig. 6.

Performance of the ANN

In order to evaluate the improvement ability of the AAN for each soft-tissue point, the improvement rates were calculated and are listed in Table 4. The improvement rate of the average error was defined as:

$$\frac{|\text{average error of prediction}| - |\text{average error of improved prediction}|}{|\text{average error of prediction}|} \times 100\%$$

The improvement rate of the SD was defined as:

$$\frac{|\text{SD of prediction error}| - |\text{SD of improved prediction error}|}{|\text{SD of prediction error}|} \times 100\%$$

On the sagittal plane, the lower face region showed better improvement when compared with all samples. The improvement rates exceeded 80%. Soft-tissue A and B points were the most greatly improved and showed 100% improvement rates. This means that the prediction errors were eliminated,

Table 4. Improvement rate

	Sagittal plane		Vertical plane	
	Avg (%)	Std (%)	Avg (%)	Std (%)
Compared with all samples				
Tip of the nose	−40.0	−25.0	+80.0	−20.0
Subnasale	−41.2	+47.6	−25.0	+6.7
Soft-tissue A point	+100.0	+40.0	+80.0	+57.7
Upper lip	+25.0	+63.0	+64.7	+62.5
Lower lip	+80.0	+56.5	+66.7	+66.7
Soft-tissue B point	+100.0	+46.7	−400.0	+47.1
Soft-tissue pogonion	+83.3	+71.9	+87.5	+81.1
Compared with Group B				
Tip of the nose	0.0	0.0	+66.7	+5.3
Subnasale	−20.0	+56.0	−25.0	−7.7
Soft-tissue A point	+100.0	+40.0	+66.7	+56.0
Upper lip	+14.3	+56.5	+50.0	+47.1
Lower lip	+77.8	+58.3	+80.0	+68.4
Soft-tissue B point	+100.0	+36.0	+44.4	+41.9
Soft-tissue pogonion	+33.3	+75.7	+88.9	+73.1

Avg = improvement rate of the average error; Std = improvement rate of the standard deviation.

and the average error was 0. The improvement rate of the least accurate point, the lower lip, was 80%. The improvement rates of the tip of the nose and subnasale were negative and showed that the improvement actually made them less accurate. Most SDs of the soft-tissue points improved except for the tip of the nose. The soft-tissue point that possessed the largest SD, the soft-tissue pogonion, had the highest improvement rate of the SD. The improvement rates of the upper and lower lips exceeded 50%. On average, the improvement rate of the average error on the sagittal plane was 43.9%, and that of the SD was 42.9%.

On the vertical plane, the soft-tissue pogonion, the soft-tissue A point, and the tip of the nose possessed the largest improvement rate of average errors when compared with all samples. The improvement rates of these points exceeded 80%. The most greatly improved point was the soft-tissue pogonion which showed 87.5% improvement. The improvement rate of the least accurate point, the upper lip, was 64.7%. The improvement rate of the most accurate point, the soft-tissue B point, was −400%. The improvement rate of the SD of the soft-tissue pogonion was the highest, while that of the tip of the nose was the lowest. The improvement rate of the average error of the tip of the nose was 80%; however, the improvement rate of the SD was −20%. This shows that the range of the error distribution was wider after improvement at this soft-tissue point. On average, the improvement rate of the average error on the vertical plane was −6.6%, and the improvement rate of the SD was 43.1%.

Generally, the overall improvement rate of the average error was 18.7%, and the overall improvement rate of the SD was 43.0%.

Discussion

The basic model of ANNs was proposed by Warren McCulloch (a neurologist) and Walter Pitts (a mathematician) in 1943.[27] They developed a neural network using simple binary threshold functions. According to Mitchell,[28] ANNs provide powerful tools to approach real situations by learning examples. They provide powerful effects in visual recognition, acoustic recognition, and image recognition. They are able to find useful information among original data and establish a model for decision making and results prediction. A feed-forward back-propagation learning ANN[29] was used in this study. Such networks are made up of layers of neurons, typically an input layer, one or more hidden layers, and an output layer. Each layer is fully connected to the other layers. The neurons are connected by links that are associated with numerical weightings. A neural network learns from its experience in a training environment through repeated adjustments of these weightings.

ANNs are widely used in medical research.[30–39] Folland et al.[31] used an ANN to discriminate cardiac sounds. They used multilayer perceptron and radial basis function for their neural network. The results showed that the abilities to discriminate abnormal cardiac sounds were 84% and 88%. Spicker et al.[32]

predicted the sequence of human p53 tumor suppressor gene with an ANN. Ortolani et al.[33] used an ANN to monitor changes in electroencephalographs (EEGs) in order to determine the anesthetic depth of patients. The EEGs of 150 patients were used for the input data, and the anesthetic depth judged by the anesthetist was used as the target set. Another 50 patients were used to test the system, and they found that this ANN was able to detect the anesthetic depth of patients. Baxt et al.[34] used an ANN to quickly diagnose patients with chest pain and discriminate ones with acute cardiac infarction. They trained the ANN with 2204 patients with chest pain and a final diagnosis. The symptoms and signs of another 128 patients with acute cardiac infarction were input into the system, and 121 patients were correctly diagnosed. They concluded that this system was useful for preliminarily diagnosing patients in the emergency room. Lo et al.[37] predicted breast cancer invasion with ANNs. Nine mammographic findings and patient age were used as input data, and the results of a biopsy were used as the output data. They found that the specificity of this system was 100% and the sensitivity was 71%, and thought this knowledge might help in surgical planning and to reduce the costs and morbidity of unnecessary biopsies. In dentistry, ANNs are also used for diagnosis and screening. Devito et al.[38] used an artificial multilayer perceptron neural network to diagnose proximal caries. They trained the network with 160 radiographic images and found that the diagnostic improvement using the neural network was 39.4%. The results were better than the average of the examiners. Radke et al.[39] differentiated normal temporomandibular joints and non-reducing displaced disks with an ANN. All normal subjects were detected as normal patients with 100% specificity, while 86.8% of patients were correctly classified. Speight et al.[30] utilized an ANN for oral cancer screening; they trained the network with 1662 samples and used another 365 samples for the test. They found the sensitivity to be 0.80 and the specificity to be 0.77. For general dentists, the screening sensitivity was 0.74 and the specificity was 0.99. The authors thought that this ANN was applicable considering the costs.

According to research by Romani et al.[40], nearly 50% of orthodontists surveyed could not detect changes of 2 mm in vertical movement of the maxilla. In the present study, 2 mm was chosen as the threshold of tolerance for improved prediction error in order to establish the target set of the ANN. To set up the sequence of the soft-tissue check points when modifying hard-tissue movements, the less accurate points were improved first. In this study, the lower lip and chin region was a less accurate region and the upper lip and nose region was a relatively accurate region. Thus, the sequence of soft-tissue check points began from Pg′ then LL, B′, UL, A′, Sn, and ended at Prn.

Although ANNs are widely used in the fields of both medicine and dentistry, they are mainly used in decision making, diagnosis, and prognosis prediction.[24] No article regarding improving postsurgical facial profile imaging predictions was found during a literature review. Thus, comparisons with similar studies in the literature are difficult to make. However, the present study shows another potential application of ANNs in dentistry.

The results of the present study confirmed that ANNs are able to improve the postsurgical facial profile prediction to a clinically applicable level. After the improvement by the ANN, most of the prediction errors were <1 mm, except for the subnasale. The improvement rate of the subnasale was also the worst among the evaluated soft-tissue landmarks. A similar situation was found at the tip of the nose. This might have been due to the method of gaining the target set in this study. In this study, the movement of hard tissue was adjusted in order to make the prediction more accurate. After one soft-tissue point achieved a prediction error of <2 mm by changing the hard-tissue movement, we went to the next soft-tissue point. It is possible that we adjusted the prediction error of the present soft-tissue point to <2 mm but made the prediction error of the previous soft-tissue points >2 mm. In our protocol, this change would be abandoned, and all prediction errors of the previous soft-tissue points should remain <2 mm. The sequence of the adjustments was the soft-tissue pogonion, the lower lip, soft-tissue B point, the upper lip, soft-tissue A point, the subnasale, and the tip of the nose. The prediction error of the nose region was of least concern, and this might have led to less improvement or even a worse prediction.

From the scattergrams, we found that the improved prediction errors were concentrated in the origin of the coordinate and/or to the center of original prediction errors. It seemed that the improvement in the ANN was to eliminate the most dispersed points and become concentrated at the center of the distribution and the origin of the coordinates.

On the vertical plane, the improvement rate of the most accurate point, soft-tissue B point, was −400%. The improvement rate of this point seemed to be very poor; however, the average prediction error of this point after improvement was rather small (0.5 mm). When compared with Group B samples only, the improvement rate was 44% (Table 4). This might have been due to the average prediction error of the soft-tissue B point of all samples

being smaller than that of Group B, thus the value of the improvement rate was negative.

In this study, the target set of the ANN was obtained by manual adjustment. This means that the intelligence of the operator to make the predicted image more similar to the final actual image was transplanted to the artificial network. The artificial networks process this intelligence with mathematical variables which are optimized during the training process. According to Scott et al.[41], the accuracy of the new predictions of the artificial network depends upon the completeness of the training process and the degree to which the training cases represent the population for which the network will be used. Because of the limited sample size in this study, the manual adjustment was repeated three times in order to provide more training samples for the ANN. The repeated manual adjustment of a specific case might be similar; however, it was regarded as an independent case, because each adjustment provided the independent prediction intelligence and a representative population for the ANN.

Because of limitations of the prediction software, the hard-tissue movement of the ANS, Pog, lower incisor root apex, angle of upper incisor to the SN plane, and lower incisor mandibular plane angle were the only values we were able to modify and improve the predictions. The prediction might be more accurate and reliable if more variables, such as surgical and orthodontic methods, were able to be input to and adjusted by the ANN.

Conclusion

1. The tip of the nose and the upper lip were the most reliable areas when using the video simulation to predict the postsurgical outcomes with bimaxillary protrusion surgery.
2. The prediction of the lower lip was the least accurate area and tended to underestimate the amount of soft-tissue retraction.
3. The frequency of the overall prediction errors of <2 mm without improvement was 52%.
4. With the improvement of the ANN, the average prediction errors and SDs were smaller, and the error distribution became more concentrated.
5. With the improvement of the ANN, the frequency of the overall prediction errors of <2 mm was 84.5%.
6. The improvement rates of the ANN were 18.7% for average errors and 43.0% for the SDs.
7. The ANN possesses the ability to improve the postsurgical video image profile predictions to a clinically applicable and treatment planning level.

References

1. Kiyak HA, Bell R. Psychosocial considerations in surgery and orthodontics. In: Proffit WR, White RP, eds. *Surgical Orthodontic Treatment*. St Louis, MO: Mosby-Year Book, 1991:71–95.
2. Ackerman JL, Proffit WR. Communication in orthodontic treatment planning: bioethical and informed consent issues. *Angle Orthod* 1995;65:253–61.
3. Turpin DL. The need for video imaging. *Angle Orthod* 1995; 65:243.
4. Proffit WR. Treatment planning: the search for wisdom. In: Proffit WR, White RP, eds. *Surgical Orthodontic Treatment*. St Louis, MO: Mosby-Year Book, 1991:142–91.
5. Cohen MI. Mandibular prognathism. *Am J Orthod* 1965;51: 368–79.
6. McNeil RW, Proffit WR, White RP. Cephalometric prediction for orthodontic surgery. *Angle Orthod* 1972;42:154–64.
7. Henderson D. The assessment and management of bony deformities of the middle and lower face. *Br J Plast Surg* 1974;27:287–96.
8. Sarver DM, Johnston MW, Matukas VJ. Video imaging for planning and counseling in orthognathic surgery. *J Oral Maxillofac Surg* 1988;46:939–45.
9. Sarver DM, Johnston MW. Video imaging: techniques for superimposition of cephalometric radiography and profile images. *Int J Adult Orthodon Orthognath Surg* 1990;5:241–8.
10. Sarver DM, Matukas VJ, Weissman SM. Incorporation of facial plastic surgery in the planning and treatment of orthognathic surgical cases. *Int J Adult Orthodon Orthognath Surg* 1991;6:227–39.
11. Lew KK. The reliability of computerized cephalometric soft tissue prediction following bimaxillary anterior subapical osteotomy. *Int J Adult Orthodon Orthognath Surg* 1992;7: 97–101.
12. Takahashi I, Takahashi T, Hamada M, et al. Application of video surgery to orthodontic diagnosis. *Int J Adult Orthodon Orthognath Surg* 1989;4:219–22.
13. Turpin DL. Computers coming on-line for diagnosis and treatment planning. *Angle Orthod* 1990;60:163.
14. Laney TJ, Kuhn BS. Computer imaging in orthognathic and facial cosmetic surgery. *Oral Maxillofac Clin North Am* 1990; 2:659–68.
15. Phillips C, Hill BJ, Cannac C. The influence of video imaging on patients' perceptions and expectations. *Angle Orthod* 1995;65:263–70.
16. Lu CH, Ko EW, Huang CS. The accuracy of video imaging prediction in soft tissue outcome after bimaxillary orthognathic surgery. *J Oral Maxillofac Surg* 2003;61:333–42.
17. Sinclair PM, Kilpelainen P, Phillips C, White RP Jr, Rogers L, Sarver DM. The accuracy of video imaging in orthognathic surgery. *Am J Orthod Dentofacial Orthop* 1995;107:177–85.
18. Kazandjian S, Sameshima GT, Champlin T, Sinclair PM. Accuracy of video imaging for predicting the soft tissue profile after mandibular set-back surgery. *Am J Orthod Dentofacial Orthop* 1999;115:382–9.
19. Sameshima GT, Kawakami RK, Kaminishi RM, Sinclair PM. Predicting soft tissue changes in maxillary impaction surgery: a comparison of two video imaging systems. *Angle Orthod* 1997;67:347–54.
20. Syliangco ST, Sameshima GT, Kaminishi RM, Sinclair PM. Predicting soft tissue changes in mandibular advancement surgery: a comparison of two video imaging systems. *Angle Orthod* 1997;67:337–46.
21. Konstiantos KA, O'Reilly MT, Close J. The validity of the prediction of soft tissue profile changes after LeFort I osteotomy using the Dentofacial Planner (computer software). *Am J Orthod Dentofacial Orthop* 1994;105:241–49.

22. Hing NR. The accuracy of computer generated prediction tracings. *Int J Oral Maxillofac Surg* 1989;18:148–51.
23. Upton PM, Sadowsky PL, Sarver DM, Heaven TJ. Evaluation of video imaging prediction in combined maxillary and mandibular orthognathic surgery. *Am J Orthod Dentofacial Orthop* 1997;112:656–65.
24. Ramesh AN, Kambhampati C, Monson JR, Drew PJ. Artificial intelligence in medicine. *Ann R Coll Surg Engl* 2004;86:334–8.
25. Agatonovic-Kustrin S, Beresford R. Basic concepts of artificial neural network (ANN) modeling and its application in pharmaceutical research. *J Pharm Biomed Anal* 2000;22: 717–27.
26. Alvager T, Smith TJ, Vijai F. The use of artificial neural networks in biomedical technologies: an introduction. *Biomed Instrum Technol* 1994;28:315–22.
27. Anderson D, McNeill G. *Artificial Neural Networks Technology*. A DACS State-of-the Art Report, August 20, 1992. Available at: https://www.thedacs.com/techs/abstracts/abstract.php?dan=347002
28. Mitchell TM. Chapter 4: Artificial neural networks. In: Mitchell TM, ed. Machine Learning. New York: McGraw-Hill, 1997:81–127.
29. Werbos P. *Beyond Regression: New Tools for Prediction and Analysis in the Behavioral Sciences* [PhD thesis]. Cambridge, MA: Harvard University, 1974.
30. Speight PM, Elliott AE, Jullien JA, Downer MC, Zakzrewska JM. The use of artificial intelligence to identify people at risk of oral cancer and precancer. *Br Dent J* 1995;25;179:382–7.
31. Folland R, Hines EL, Boilot P, Morgan D. Classifying coronary dysfunction using neural networks through cardiovascular auscultation. *Med Biol Eng Comput* 2002;40:339–43.
32. Spicker JS, Wikman F, Lu ML, et al. Neural network predicts sequence of *TP53* gene based on DNA chip. *Bioinformatics* 2002;18:1133–4.
33. Ortolani O, Conti A, Di Filippo A, et al. EEG signal processing in anaesthesia: use of a neural network technique for monitoring depth of anaesthesia. *Br J Anaesth* 2002;88: 644–8.
34. Baxt WG, Shofer FS, Sites FD, Hollander JE. A neural computational aid to the diagnosis of acute myocardial infarction. *Ann Emerg Med* 2002;39:366–73.
35. Chen Y, Thosar SS, Forbess RA, Kemper MS, Rubinovitz RL, Shukla AJ. Prediction of drug content and hardness of intact tablets using artificial neural network and near-infrared spectroscopy. *Drug Dev Ind Pharm* 2001;27:623–31.
36. MacDowell M, Somoza E, Rothe K, Fry R, Brady K, Bocklet A. Understanding birthing mode decision making using artificial neural networks. *Med Decis Making* 2001;21: 433–43.
37. Lo JY, Baker JA, Kornguth PJ, Iglehart JD, Floyd CE Jr. Predicting breast cancer invasion with artificial neural networks on the basis of mammographic features. *Radiology* 1997;203:159–63.
38. Devito KL, de Souza Barbosa F, Felippe Filho WN. An artificial multilayer perceptron neural network for diagnosis of proximal dental caries. *Oral Surg Oral Med Oral Pathol Oral Radiol Endod* 2008;106:879–84.
39. Radke JC, Ketcham R, Glassman B, Kull R. Artificial neural network learns to differentiate normal TMJs and nonreducing displaced disks after training on incisor-point chewing movements. *Cranio* 2003;21:259–64.
40. Romani KL, Agahi F, Nanda R, Zernik JH. Evaluation of horizontal and vertical differences in facial profiles by orthodontists and lay people. *Angle Orthod* 1993;63:175–82.
41. Scott JA, Aziz K, Yasuda T, Gewirtz H. Integration of clinical and imaging data to predict the presence of coronary artery disease with the use of neural networks. *Coron Artery Dis* 2004;15:427–34.